

# Detailed Chemical Kinetic Modeling of Pyrolysis of Ethylene, Acetylene, and Propylene at 1073–1373 K with a Plug-Flow Reactor Model

KOYO NORINAGA,<sup>1,2</sup> VINOD M. JANARDHANAN,<sup>1</sup> OLAF DEUTSCHMANN<sup>1</sup>

<sup>1</sup>Institut für Technische Chemie und Polymerchemie, Universität Karlsruhe (TH), Engesserstr. 20, 76131 Karlsruhe, Germany

<sup>2</sup>Center for Advanced Research of Energy Conversion Materials, Hokkaido University, N13-W8, Kitaku, Sapporo 060-8628, Japan

Received 2 April 2007; revised 27 August 2007; accepted 6 November 2007

DOI 10.1002/kin.20302

Published online in Wiley InterScience (www.interscience.wiley.com).

**ABSTRACT:** This study examines the predictive capability of our recently proposed reaction mechanism (Norinaga and Deutschmann, *Ind Eng Chem Res* 2007, 46, 3547) for hydrocarbon pyrolysis at varying temperature. The conventional flow reactor experiments were conducted at 8 kPa, over the temperature range 1073–1373 K, using ethylene, acetylene, and propylene as reactants to validate the mechanism. More than 40 compounds were identified and quantitatively analyzed by on- and off-line gas chromatography. The chemical reaction schemes consisting of 227 species and 827 reactions were coupled with a plug-flow reactor model that incorporated the experimentally measured axial temperature profile of the reactor. Comparisons between the computations and the experiments are presented for more than 30 products including hydrogen and hydrocarbons ranging from methane to coronene as a function of temperature. The model can predict the compositions of major products (mole fractions larger than  $10^{-2}$ ) in the pyrolysis of three hydrocarbons with satisfactory accuracies over the whole temperature range considered. Mole fraction profiles of minor compounds including polycyclic aromatic hydrocarbons (PAHs) up to three ring systems, such as phenanthrene, anthracene, and phenyl-naphthalene, are also fairly modeled. At temperatures lower than 1273 K, larger PAHs were underpredicted and the deviation became larger with decreasing temperature and increasing molecular mass of PAHs, while better agreements were found at temperatures higher than 1323 K. © 2008 Wiley Periodicals, Inc. *Int J Chem Kinet* 40: 199–208, 2008

Correspondence to: Koyo Norinaga; e-mail: norinaga@eng.hokudai.ac.jp.  
© 2008 Wiley Periodicals, Inc.

## INTRODUCTION

When heated at around 1273 K, hydrocarbon generally undergoes pyrolysis where hydrocarbons with increasing numbers of carbon atoms and aromatic rings are progressively formed, and theoretically they convert almost completely into solid carbon and gaseous hydrogen at equilibrium [1]. The carbon formation from gaseous light hydrocarbons has both detrimental and positive aspects. The former is catalyst deactivations by coke formations [2–4]. The latter is syntheses of carbon materials such as carbon–carbon composites [5] by utilizing a chemical vapor deposition (CVD) technique. This study is performed at conditions relevant to the CVD of carbon in which a great variety of hydrocarbons and hydrocarbon radicals are formed by gas-phase reactions, and any of these species has a potential to chemisorb or physisorb at the growing solid carbon surface [6]. The mechanism of carbon formation from gas phase is still obscure, since underlying chemistry is quite complex involving both gas phase and surface.

We conducted an experimental study on a detailed product analysis of the pyrolysis of ethylene, acetylene, and propylene [7], because quantitative experimental data on the hydrocarbon pyrolysis with a wide range of product analysis including large polycyclic aromatic hydrocarbons (PAHs) had been still limited. The experiments were performed with a conventional flow reactor at conditions relevant to the CVD of pyrolytic carbon, i.e., at 1173 K and pressure from 2 to 15 kPa. Gas-phase components were analyzed by both on- and off-line gas chromatography. More than 40 compounds including hydrogen and hydrocarbons from methane to coronene were identified and quantitatively determined as a function of the residence time varied up to 1.6 s. Product recoveries were generally more than 90%, providing a useful experimental database for kinetic-modeling studies of gas-phase reactions with detailed chemistry.

We developed a gas-phase reaction mechanism consisting of 227 species and 827 reactions [8], which was evaluated using a software package for time-dependent homogeneous reaction systems. Comparisons between the experiments and computations for more than 30 compounds showed that the mechanism has a comprehensive capability in predicting concentration profiles of major components found in the pyrolysis of three different hydrocarbons with an acceptable level of accuracy, although disagreements are still observed for minor species, especially for PAHs, for which formations are underpredicted. Obvious shortcomings of the previous work [8] were the model validation at only

a single temperature (1173 K) and the computation without a transport model.

In this study, we examine the predictive capability of our recently developed mechanism at varying temperature. Pyrolysis experiments were performed using the same flow reactor at pressure of 8 kPa, residence time of 0.5 s, and over the temperature range of 1073–1373 K. Numerical simulation is conducted with a software package, which can couple the detailed chemical reaction schemes with a plug-flow reactor model, in which the temperature profiles along the reactor are adequately incorporated.

## EXPERIMENTAL

The experimental data for the model validation are obtained using a vertical flow reactor with a total length of 440 mm as shown in Fig. 1 (left). The reactor employed here is identical with that used in previous CVD experiments [9]. A channel structure, made out of cordierite, with 400 channels per square inch, is fitted in an alumina ceramic tube (22-mm i.d. and 40 mm long), which is located at the center of the reactor and called the

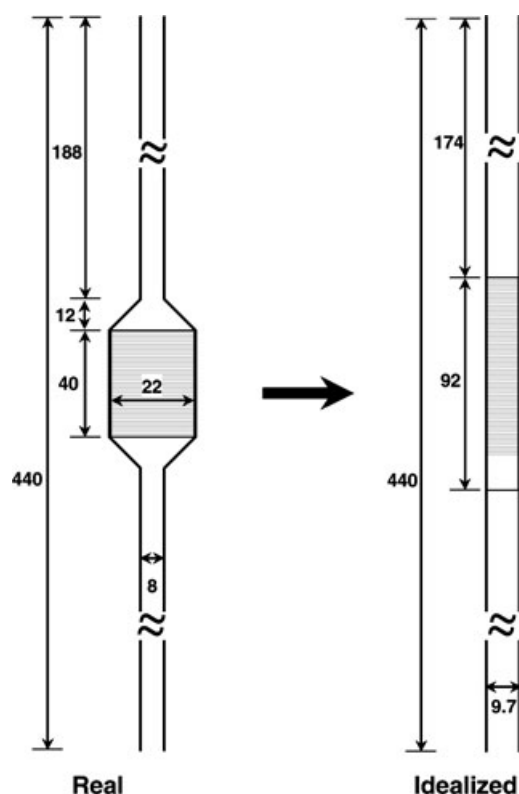


**Figure 1** Schematic diagrams of the real reactor (left) and the reactor idealized for a plug-flow simulation (right); unit: mm.

deposition space. The inlet and outlet tubes (8-mm i.d.) are connected to the deposition space through conical nozzles. The temperature of the deposition space was varied in the range between 1073 and 1373 K. Temperature profile for the reactor was measured under an argon flow with a type K thermocouple (Rössel Messtechnik GmbH & Co.) that was moved axially along the reactor length.

Ethylene, acetylene, and propylene, purchased from Air Liquide Co. Ltd., were used as source hydrocarbons. The purities of the source hydrocarbons and the initial compositions used in the computations are summarized in our previous work [8]. The pressure was maintained at 8 kPa without inert diluent gas. The flow rate of inlet source gas was controlled so that the space-time at the isothermal zone was fixed to 0.5 s. In the determination of the inlet velocity, the density change of the flowing gas by chemical reactions was not considered.

The products were analyzed by both on- and off-line gas chromatography. Gaseous products up to C<sub>4</sub> compounds were analyzed on-line with a Sichromat 3 gas chromatograph (Siemens) equipped with a vacuum-dosing system. A Porapak N column (Chrompak) and a thermal conductivity detector were used for separation and peak detection, respectively. We conducted GC measurements for gaseous products with two different modes, one for measurements of hydrogen and C<sub>1</sub>–C<sub>2</sub> hydrocarbons using argon as a carrier gas, and the other for C<sub>3</sub>–C<sub>4</sub> hydrocarbons using hydrogen as a carrier gas. Liquid products larger than benzene were collected in two cold traps set at 195 K, dissolved in a measured amount of acetone and analyzed by a Sichromat 1-4 gas chromatograph (Siemens) equipped with a capillary column (CP-Sil 8 CB LB/MS, Chrompak) and a flame ionization detector. Species were identified by the retention time matching. The estimated uncertainties in determining the concentrations of gaseous, major condensing products, and minor condensing products (mainly PAHs) were ±9%, ±28%, and ±32%, respectively. The detailed descriptions of the experimental setup and product analysis are given elsewhere [7].

## MODELING

### Mechanism

The gas-phase reaction mechanism used in this study consists of 227 species and 827 elementary reactions, of which 798 reactions are reversible. No adjustments were made to the kinetic parameters of any chemical reaction. The mechanism, the reference of each of elementary reactions, the thermodynamic

data for all species and the species abbreviations, and the corresponding chemical formula are given in the previous work [8] and can also be downloaded ([www.detchem.com](http://www.detchem.com)). The conversion of source hydrocarbon into the solid carbon is generally a few percent (C<sub>1</sub> base) for ethylene and propylene, but it accounts for several percent for acetylene [9]. The development of surface reaction mechanism is currently in progress for more accurate description of the overall process in the reactor.

The appropriate treatment of pressure-dependent reactions such as dissociation and recombination reactions is important in this study because the pyrolysis experiments run at low pressures where the pressure has a significant effect on the rate constant. The mechanism involves 33 reactions with third-body species, and 31 reactions of which are given using the so-called Troe parameters [10–13]. The impact of the pressure in the comparisons of experiment and prediction data was examined in our previous paper at 1173 K and pressures ranged from 2 to 15 kPa [8]. It was found that the kinetic model adequately captures the trends of the pressure effect for major species; an increase in pressure enhances consumption of source hydrocarbons and also enhances product formation. This suggests that at least a portion of pressure-dependent reactions that are sensitive for the formation/consumption of the major species is treated adequately in the current kinetic model, although not all of pressure-dependent reactions are provided with third-body species or the Troe parameters.

### Reactor Idealization

Figure 1 shows schematic diagrams of the real reactor (left) and idealized reactor (right). The real reactor was idealized to a tube reactor with a constant inner diameter for one-dimensional plug-flow simulation so that introduced gas experiences the same temperature history as it does in the real reactor. The idealized reactor has the same length of the real reactor, and its inner diameter was determined to make it to have the same total volume of the real reactor. The length of the deposition space of the idealized reactor was determined to make it to have the same volume of that of the real reactor. This idealization is valid as long as laminar flow is maintained throughout the reactor. The flow characteristics in the same reactor were studied with a 1:1 acrylic-glass model [14], in which an ammonium chloride smoke gas was used for flow visualization. It was shown that a clear plug-flow profile was generated by the conical nozzles, which avoid an occurrence of turbulent flow at the reactor parts of varying tube diameter.

## Plug-Flow Computation

The calculations were performed using the gas-phase reaction mechanism with the PLUG code in the DETCHEM program package (DETHCEM<sup>PLUG</sup>) [15]. The DETCHEM<sup>PLUG</sup> is designed for nondispersive one-dimensional flow of chemically reacting ideal gas mixture under steady-state conditions. The system of differential algebraic equations describing the plug-flow reactor consists of the continuity equation

$$A_c \frac{d(\rho u)}{dz} = A_s \sum_{k=1}^{K_g} \dot{s}_k M_k$$

the species conservation equation

$$A_c \frac{d(\rho u Y_k)}{dz} = M_k (A_s \dot{s}_k + A_c \dot{\omega}_k)$$

the energy equation

$$\rho u A_c \frac{d(C_p T)}{dz} + \sum_{k=1}^{K_g} \dot{\omega}_k h_k M_k A_c + \sum_{k=1}^{K_g} \dot{s}_k h_k M_k A_s = U A_s (T_w - T)$$

and the equation of state

$$p \bar{M} = \rho R T$$

In the above equations,  $\rho$  is the density,  $u$  is the velocity,  $A_c$  is the area of cross section of the channel,  $A_s$  is the surface area per unit length,  $K_g$  is the number of gas-phase species,  $\dot{s}_k$  is the molar rate of production

of species  $k$  by surface reaction,  $\dot{\omega}_k$  is the molar rate of production of species  $k$  by the gas-phase reaction,  $M_k$  is the molecular mass of species  $k$ ,  $Y_k$  is the mass fraction of species  $k$ ,  $C_p$  is the specific heat capacity of species  $k$ ,  $h_k$  is the specific enthalpy of species  $k$ ,  $U$  is the overall heat transfer coefficient,  $T_w$  is the wall temperature,  $T$  is the gas temperature,  $p$  is the pressure, and  $\bar{M}$  is the average molecular weight. However, since the study carried out here does not account for surface reactions, all the terms containing the term  $\dot{s}_k$  vanishes. Furthermore, the energy equation is not solved since the measured temperature profile in the reactor is incorporated into the code using a separate subroutine. However, the equation is given here for the sake of completeness. The system of equations is solved using the differential algebraic equation solver LIMEX.

The measured (symbols) and modeled (lines) temperature profiles of the reactor are shown in Fig. 2. The linear lines connecting the neighboring points correspond to the temperature profile input for the computations. The other input parameters were obtained from the experimental conditions such as inlet velocity, molar composition, pressure, and so on. The computations were performed for seven different temperature profiles with the temperature at quasi-isothermal zone ranging from 1073 to 1373 K.

The gas temperature profile inside the reactor was also examined by numerical simulations with a two-dimensional reactor model using DETCHEM<sup>CHANNEL</sup> [15]. A laminar flow model is coupled with the detailed chemical reaction schemes identical to that used in the present study. The simulation shows that gas temperature is almost uniformly distributed in the radial

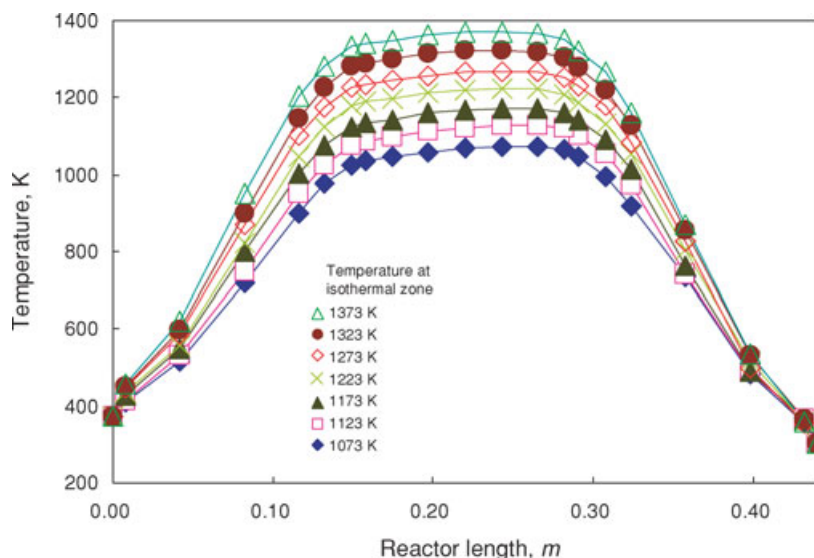


**Figure 2** Experimentally obtained temperature profiles along the reactor at seven temperatures of the quasi-isothermal zone. The measured points are connected by linear lines and used for the DETCHEM<sup>PLUG</sup> simulations. [Color figure can be viewed in the online issue, which is available at [www.interscience.wiley.com](http://www.interscience.wiley.com).]

direction along the quasi-isothermal zone of the reactor when the inner diameter of the tube equals to that of the reactor used in this study. Hence, errors in numerical simulations with neglecting radial temperature distribution should be minimal.

### Reaction Pathway Analysis

Reaction pathways leading to benzene were analyzed to identify crucial reactions for benzene formation and to assess the effect of temperature on the contributions of individual reactions. Rates of formation for species such as benzene and the precursors were determined using a rate analysis code included in the HOMREA software package [16]. The reaction pathway analysis was performed at a condition of  $p = 8$  kPa, residence time = 0.5 s, and temperatures from 1073 to 1373 K.

## RESULTS OF COMPUTATIONS

### Velocity of Chemically Reacting Flow along the Reactor

Figure 3 shows the wall temperature profile in which the quasi-isothermal zone temperature is 1273 K used for the computations (upper) and the computational outputs for the velocity profiles for ethylene, acetylene, and propylene pyrolysis (lower) along the reactor length. Up to the reactor length of 0.12 m, all gases exhibit the same velocity profiles and their trends are exactly same as the wall temperature profiles. This indicates that the velocity increase, in other words the density decrease, is induced simply by the temperature effect. Chemical reactions changing the fluid density are here negligible. Beyond 0.12 m, at which the wall temperature is 1120 K, three gases show different velocity profiles. Rapid velocity increases are observed for propylene and ethylene demonstrating that these gases undergo pyrolysis reactions dominated by decompositions, which lead to density decrease. On the other hand, the velocity of acetylene shows an incipient small increase and then gradually decreases. This indicates that the acetylene pyrolysis is primarily dominated by recombination reactions leading to density increase. After the reactor length of 0.29 m, velocities of three gases decrease with decreasing temperature. The velocity at the reactor outlet is in the order of propylene > ethylene > acetylene. These simulation results well correspond to our previous experimental results on the velocity measurements at the reactor outlet [7].

### Gas-Phase Composition along the Reactor

Figure 4 shows the computed mole fraction profiles of major compounds in the pyrolysis of (a) ethylene,

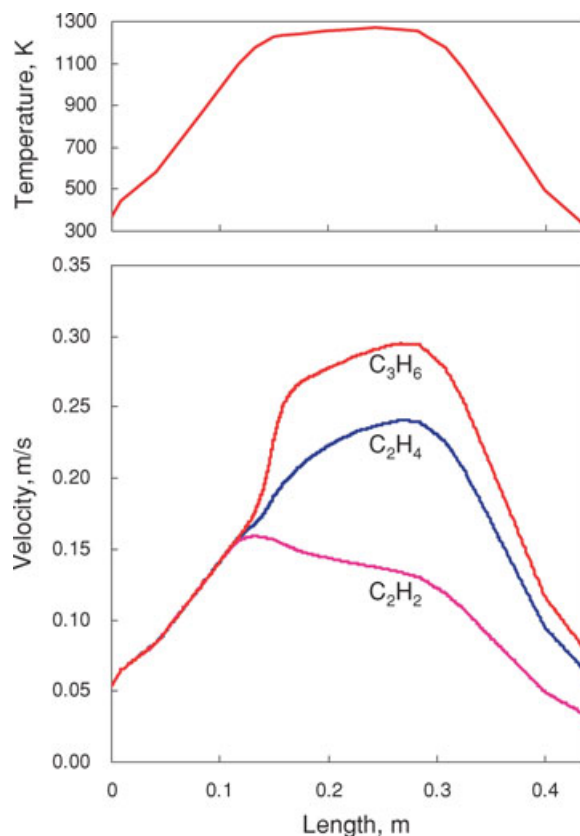


**Figure 3** Wall temperature profile in which the quasi-isothermal zone temperature is 1273 K used for the computations (upper) and the computational outputs for the velocity profiles in the ethylene, acetylene, and propylene pyrolysis (lower) along the reactor length. [Color figure can be viewed in the online issue, which is available at [www.interscience.wiley.com](http://www.interscience.wiley.com).]

(b) acetylene, and (c) propylene at the isothermal zone temperature of 1273 K. At 0.12 m, all source gases start to destruct and various products start to form. C<sub>4</sub> species such as vinylacetylene and 1,3-butadiene as well as C<sub>3</sub> species such as propyne and propadiene exhibit intermediate behaviors of which concentrations go through maxima at short reactor length. Little changes in any species' concentration occur beyond 0.3 m due to the temperature drop.

## COMPARISONS OF EXPERIMENTS AND COMPUTATIONS

### Major Compounds

Figures 5–7 compare the computational predictions at the reactor outlet (length = 0.44 m) with the experimental data for major compounds (mole fractions > 10<sup>-3</sup>) as a function of the quasi-isothermal zone temperature. In general, the major species predictions

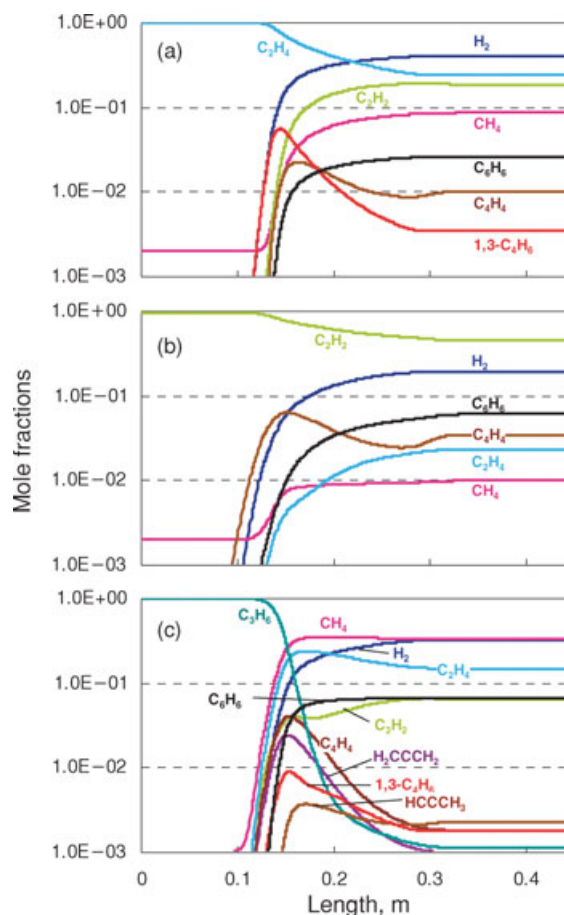


**Figure 4** Computed mole fraction profiles of major compounds in the pyrolysis of (a) ethylene, (b) acetylene, (c) and propylene at the isothermal zone temperature of 1273 K, pressure of 8 kPa, and reactant inlet velocity of 0.05 m/s. [Color figure can be viewed in the online issue, which is available at [www.interscience.wiley.com](http://www.interscience.wiley.com).]

agree well with the experimental data over the whole temperature range, considering that the model parameters were never fitted to match the experimental data. Exceptions are the intermediate species such as 1,3-butadiene for ethylene pyrolysis and vinylacetylene for both ethylene and acetylene pyrolysis, which are overpredicted by factors of 3–4, but their trends are captured well. The hydrogen mole fraction in acetylene pyrolysis at high temperatures ( $\gg 1223$  K) is underpredicted by about 35–100%. Carbon deposition from hydrocarbon always accompanies hydrogen formation. The exclusion of heterogeneous reactions in the present simulation results in the significant disagreements in hydrogen formation from acetylene, which has the highest propensity to form carbon deposit among three hydrocarbons examined [9].

The model can predict the profiles of major products in the pyrolysis of three hydrocarbons with satisfactory accuracies over the whole temperature range consid-

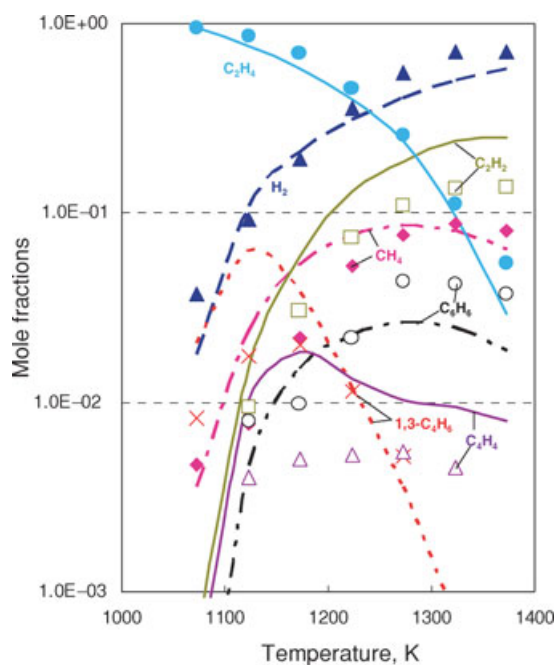
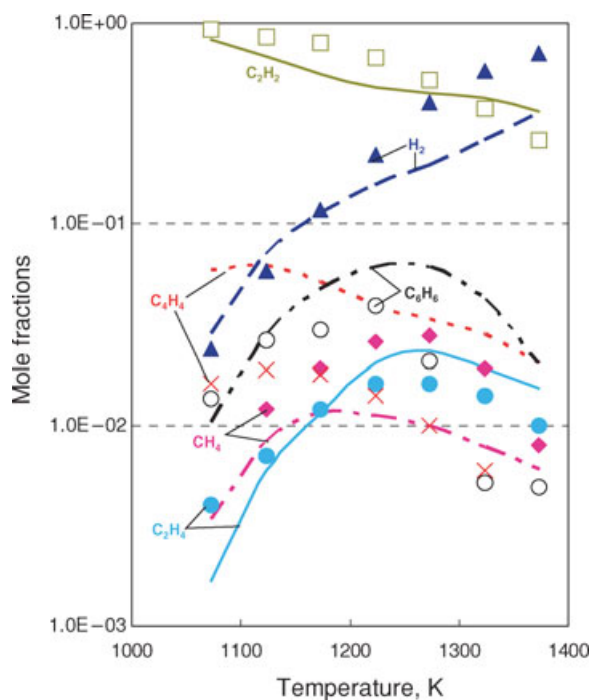


**Figure 5** Comparison of the computational predictions at the reactor outlet (length = 0.44 m) with the experimental data for major compounds (mole fractions  $> 10^{-3}$ ) in ethylene pyrolysis at 8 kPa as a function of the quasi-isothermal zone temperature. Lines and symbols are the predictions and the experiments, respectively. [Color figure can be viewed in the online issue, which is available at [www.interscience.wiley.com](http://www.interscience.wiley.com).]

ered when the space-time at quasi-isothermal zone is fixed to 0.5 s. The residence time is an important parameter to consider. Although the impact of residence time on the comparison between the model and the experiments was thoroughly examined at 1173 K [8], this does not guarantee that the present kinetic model can predict successfully the pyrolysis behaviors of the three hydrocarbons over a range of residence time at other temperatures.

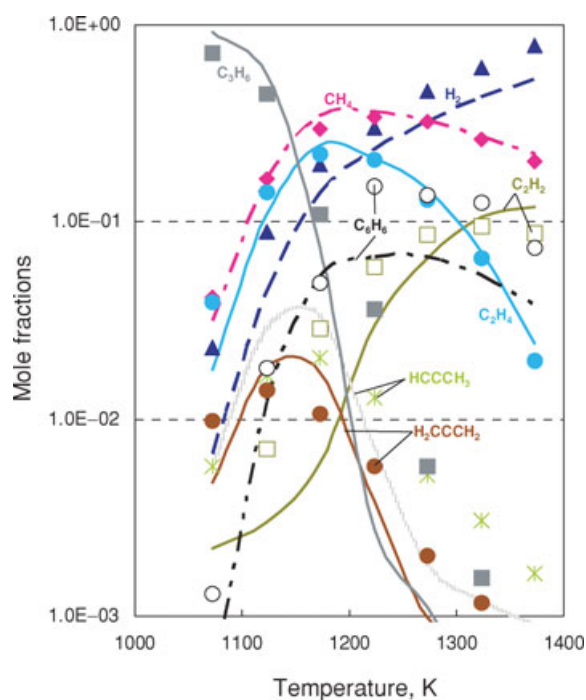
### Minor Compounds

Figure 8 presents the computational and experimental mole fractions of minor compounds in the ethylene pyrolysis. The minor compounds are classified into  $C_3$ ,  $C_4$  hydrocarbons (upper), benzene substitutes (middle), and compounds with two rings and acenaphthylene (bottom). Vinylacetylene is  $\sim 3$ -fold overpredicted, but the profiles of other species are fairly predicted and their trends are well captured. For the benzene substitutes, an overprediction ( $\sim 3$ -fold) of styrene at low temperatures is observed. All the prediction curves show maxima, and the same trends are observed experimentally for toluene and styrene, though the mole fraction peaks appear at higher temperatures



**Figure 6** Comparison of the computational predictions at the reactor outlet (length = 0.44 m) with the experimental data for major compounds (mole fractions  $>10^{-3}$ ) in acetylene pyrolysis at 8 kPa as a function of the quasi-isothermal zone temperature. Lines and symbols are the predictions and the experiments, respectively. [Color figure can be viewed in the online issue, which is available at [www.interscience.wiley.com](http://www.interscience.wiley.com).]

than those by predictions. Experimental mole fraction of phenylacetylene increases monotonously with increasing temperature unlike the prediction. The reaction pathway analysis shows that phenylacetylene is consumed almost solely by phenylacetylene + H  $\rightarrow$  C<sub>6</sub>H<sub>5</sub> (phenyl radical) + acetylene at 1073 K. With increasing temperature, contribution of this reaction is decreased instead the contributions of phenylacetylene + C<sub>2</sub>H<sub>3</sub>  $\rightarrow$  C<sub>6</sub>H<sub>5</sub> + vinylacetylene and phenylacetylene + phenyl  $\rightarrow$  phenanthrene + H become significant. The pathway analysis also indicates that styrene dehydrogenation (styrene + H  $\rightarrow$  C<sub>6</sub>H<sub>5</sub>CCH<sub>2</sub> + H<sub>2</sub> and C<sub>6</sub>H<sub>5</sub>CCH<sub>2</sub> + H  $\rightarrow$  phenylacetylene + H<sub>2</sub>) is the preferred phenylacetylene production route over the temperature range examined. With increasing temperature, the C<sub>6</sub>H<sub>5</sub> + acetylene  $\rightarrow$  phenylacetylene + H pathway becomes important and contributes about 20% of the phenylacetylene formation at 1373 K. The examinations of the rate and thermodynamic parameters of the above-mentioned reactions may improve the prediction of the phenylacetylene concentration. On the experimental side, the quantification of phenylacetylene should be further examined since it is hard



**Figure 7** Comparison of the computational predictions at the reactor outlet (length = 0.44 m) with the experimental data for major compounds (mole fractions  $>10^{-3}$ ) in propylene pyrolysis at 8 kPa as a function of the quasi-isothermal zone temperature. Lines and symbols are the predictions and the experiments, respectively. [Color figure can be viewed in the online issue, which is available at [www.interscience.wiley.com](http://www.interscience.wiley.com).]

to separate the peaks from xylene, ethylbenzene, and phenylacetylene in our current GC measurement. The agreements for the other species would generally be acceptable except for a significant overprediction of biphenyl (by a factor of about 40) at lower temperature, considering that the absolute concentration values are as small as  $10^{-6}$  to  $10^{-3}$ . Similar results obtained for the minor products in acetylene and propylene pyrolysis are given in the Supporting Information.<sup>1</sup>

### Polycyclic Aromatic Hydrocarbons

The computational and experimental mole fractions of large PAHs ( $\geq$  phenanthrene) are shown in Fig. 9 for acetylene pyrolysis. The same figures for other two hydrocarbon sources (ethylene and propylene) are given in the Supporting Information. Mole fraction profiles of PAHs such as phenanthrene, anthracene, phenyl-naphthalene, and fluoranthene are fairly predicted. At temperatures lower than 1273 K, larger PAHs are

<sup>1</sup>Supplementary information is available at <http://www.interscience.wiley.com/jpages/0538-8066/suppmat/>.

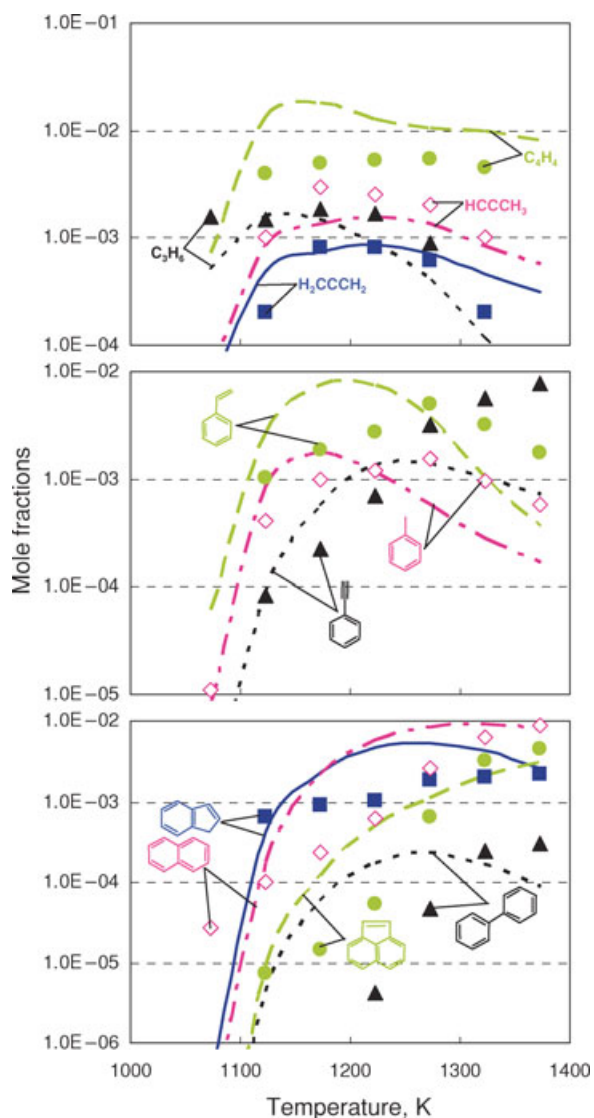


**Figure 8** Comparison of the computational predictions at the reactor outlet (length = 0.44 m) with the experimental data for minor compounds in ethylene pyrolysis at 8 kPa as a function of the quasi-isothermal zone temperature. Lines and symbols are the predictions and the experiments, respectively. [Color figure can be viewed in the online issue, which is available at [www.interscience.wiley.com](http://www.interscience.wiley.com).]

underpredicted. The deviations appear to be larger with decreasing temperature and increasing molecular mass of PAHs. The underpredictions of 2–5 orders of magnitude are observed at low temperatures. These gaps become smaller with increasing temperature, and better agreements are obtained at temperature larger than 1323 K. The PAHs formation mechanism is acquired from the high-temperature flame modeling study by Richter and Howard [17] and would be applicable only at high temperature. Further explorations of new routes to PAHs as well as improvements of kinetic parameters of the reactions sensitive to PAHs concentrations

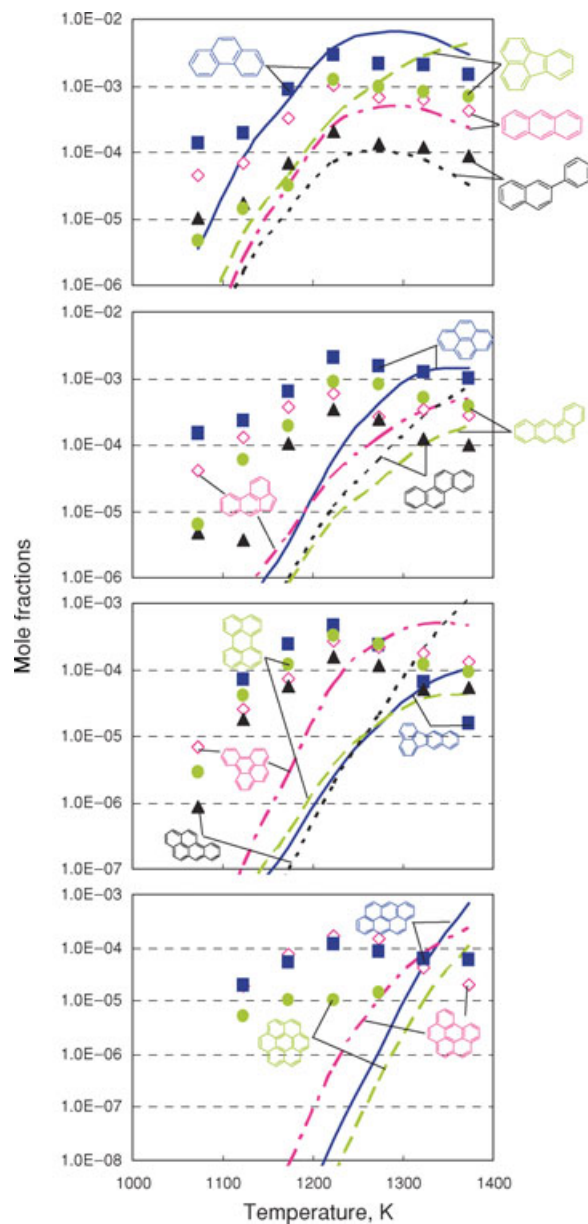


**Figure 9** Comparison of the computational predictions at the reactor outlet (length = 0.44 m) with the experimental data for polycyclic aromatic hydrocarbons in acetylene pyrolysis at 8 kPa as a function of the quasi-isothermal zone temperature. Lines and symbols are the predictions and the experiments, respectively. [Color figure can be viewed in the online issue, which is available at [www.interscience.wiley.com](http://www.interscience.wiley.com).]

would help to close the gaps at the lower temperature. Nevertheless, the increasing gap with increasing PAHs sizes and decreasing temperature strongly suggests the further necessity of incorporation of the transport model such as molecular diffusion of the species in both axial and radial directions. The present pyrolysis experiments were carried out at reduced pressures and relatively low flow rates with no carrier gas.

Under such conditions, the fluid has very low Reynolds numbers. An axial diffusion [18] is then likely to have a significant effect on the overall flow characteristics in the reactor.

## ANALYSIS OF REACTION PATHWAYS LEADING TO BENZENE

The results of the reaction pathway analysis for the major species at 1173 K were reported in the previous paper [8], and the major reaction routes to benzene were identified. Here the effect of temperature on the contributions of the crucial reactions leading to benzene, which is the most abundant aromatics in the gas phase, is assessed.

In the ethylene pyrolysis, benzene is formed primarily by dehydrogenation of 1,3-cyclohexadiene (1,3-cyclohexadiene  $\rightarrow$  benzene + H<sub>2</sub>). The contribution of this reaction is decreased from 82% to 34% with increasing temperature from 1073 to 1373 K. Benzene is produced secondarily (~13%) by 1,3-cyclohexadienyl  $\rightarrow$  benzene + H at 1073 K, but the contribution is decreased down to 5% at 1373 K. The 1,3-cyclohexadiene is formed almost solely by isomerization of 1,3-hexatriene, which is formed also almost solely by the combination of 1,3-butadiene and vinyl radical (1,3-butadiene + C<sub>2</sub>H<sub>3</sub>  $\rightarrow$  1,3-hexatriene + H). 1,3-Cyclohexadienyl is produced from by hydrogen abstraction of 1,3-cyclohexadiene such as 1,3-cyclohexadiene  $\rightarrow$  1,3-cyclohexadienyl + H and 1,3-cyclohexadiene + H  $\rightarrow$  1,3-cyclohexadienyl + H<sub>2</sub>. These reactions dominate the 1,3-cyclohexadienyl formation at low and intermediate temperatures. Isomerization of 1-methyl-cyclopentadienyl becomes significant with increasing temperature and contributes 15% of the 1,3-cyclohexadienyl formation at 1373 K. The contribution of the cyclization of 1,3-hexadiene-5-yne (1,3-hexadiene-5-yne + H  $\rightarrow$  benzene + H) for the benzene formation is less than 10% over the temperatures examined. Instead of the formation of benzene from C<sub>6</sub> species, contributions of combinations of C<sub>3</sub> species (propadiene + C<sub>3</sub>H<sub>3</sub> (propargyl)  $\rightarrow$  benzene + H, C<sub>3</sub>H<sub>5</sub> (allyl radical) + C<sub>3</sub>H<sub>3</sub>  $\rightarrow$  benzene + H + H) and combinations of C<sub>4</sub> and C<sub>2</sub> species (vinylacetylene + acetylene  $\rightarrow$  benzene) become important with increasing temperature. The former and the latter reactions account for 10% and 11% of the benzene formation at 1373 K. Decomposition of toluene and styrene also contributes to the benzene formation at high temperatures, and the sum of their contributions to the benzene formation is 17% at 1373 K.

The chemistry of acetylene pyrolysis is simplest among the three hydrocarbons examined. The com-

bination between vinylacetylene and acetylene (vinylacetylene + acetylene  $\rightarrow$  benzene) is the major route to benzene. Vinylacetylene is formed almost solely by the dimerization of acetylene. Temperature has little effect on the reaction pathways of the benzene formation.

In the propylene pyrolysis, combinations between C<sub>3</sub> species such as C<sub>3</sub>H<sub>5</sub> (allyl radical) + C<sub>3</sub>H<sub>3</sub>  $\rightarrow$  benzene + H + H and propadiene + C<sub>3</sub>H<sub>3</sub>  $\rightarrow$  benzene + H are the major routes to benzene. Eighty-nine percent of benzene is produced by the former reaction at 1073 K, but its contribution decreases with increasing temperature and exhibits 35% at 1373 K. The latter reaction contributes a few percent of benzene formation at 1073 K, but the contribution increases with increasing temperature and is 13% at 1373 K. The other important route to benzene is 1,3-cyclohexadienyl  $\rightarrow$  benzene + H as also observed in the ethylene pyrolysis. The contribution becomes important with increasing temperature (6% at 1073 K and 17% at 1373 K). Unlike the ethylene pyrolysis, 1,3-cyclohexadienyl is formed almost solely by the isomerization of 1-methyl-cyclopentadienyl over the temperature range examined. Most of 1-methyl-cyclopentadienyl is formed by two reactions such as 1-methyl-cyclopentadiene  $\rightarrow$  1-methyl-cyclopentadienyl + H and cyclopentadienyl + CH<sub>3</sub>  $\rightarrow$  1-methyl-cyclopentadienyl + H, and their contributions are 53% and 43% at 1373 K, respectively. Temperature has little effect on the contributions of the two reactions to 1-methyl-cyclopentadienyl formation. Much abundance of cyclopentadiene, which is mainly formed by C<sub>3</sub>H<sub>5</sub> (allyl radical) + C<sub>2</sub>H<sub>2</sub>  $\rightarrow$  cyclopentadiene + H, cyclopentadienyl produced from cyclopentadiene, and methyl radical supports benzene production route through C<sub>5</sub> species in the pyrolysis of propylene. Methyl and cyclopentadienyl are important radicals as well as H radical in the propylene pyrolysis. For instance, more than 60% of allyl radical is formed by H abstraction of propylene attacked by methyl and cyclopentadienyl radicals, whereas the reaction C<sub>3</sub>H<sub>6</sub> + H  $\rightarrow$  allyl + H<sub>2</sub> contributes 25% of allyl formation at 1223 K. Considerations of H abstractions from PAHs by radicals except for H radical would improve the prediction of PAHs formation of which growth pathways are presently involved only in the hydrogen-abstraction/acetylene-addition (HACA) mechanism that was introduced in the high-temperature combustion study [19–21].

## CONCLUSION

Our recently developed gas-phase reaction mechanism for the pyrolysis of ethylene, acetylene, and propylene, which had been validated only at 1173 K, was

found to exhibit an acceptable capability in predicting the product distributions even at varying temperature ranging from 1073 to 1373 K. Advanced from the previous completely mixed reactor model (zero-dimensional simulation), the detailed chemical kinetic schemes were coupled with a plug-flow reactor model that incorporates the axial temperature profiles of the reactor. The computational predictions were compared with the experimental data obtained with a conventional flow reactor for 35 species including hydrogen and hydrocarbons ranging from methane to coronene. Such an extensive model validation was not found in other detailed chemical kinetic studies for light hydrocarbon pyrolysis [22–31]. The model can predict the profiles of major products (mole fractions larger than  $10^{-2}$ ) in the pyrolysis of three hydrocarbons with satisfactory accuracies over whole temperature range. Mole fraction profiles of minor compounds including PAHs up to three ring systems are also fairly modeled. Although the predictions are still not perfect, it is encouraging that the detailed mechanism developed by compiling elementary reactions could be verified at comprehensive operational conditions without any modification and to have a merit in its generality which is never expected in kinetic models with rate constants determined by numerical fittings. Underpredictions are observed for the larger PAHs at temperature lower than 1273 K at which the deviation becomes larger with decreasing temperature and increasing molecular mass of PAHs, while better agreements are found at temperature higher than 1323 K. Several factors such as lack of chemistry for PAHs formation, inadequate kinetic parameters for the reactions sensitive to PAHs concentrations at lower temperature, and ignorance of diffusion of species as well as surface reactions attribute to the gaps found in the PAHs concentrations. Future works will include studies with the transport model such as molecular diffusion of the species in both axial and radial directions and surface (deposition) chemistry.

This research was performed in the Sonderforschungsbereich (SFB) 551 “Carbon from gas-phase: elementary reactions, structures, materials,” which is funded by the Deutsche Forschungsgemeinschaft (DFG). The Alexander von Humboldt Foundation is acknowledged for providing a research fellowship to K. Norinaga (KN). The authors acknowledge the use of the computer program HOMREA by Prof. J. Warnatz (University of Heidelberg). KN acknowledges support from Kyoto University, ACCMS and IIMC, Computing Service Group, Grant-in-Aid for Young Scientists. We thank Mr. J. Aguilera and Prof. W. Klopfer (University of Karlsruhe) for providing kinetic data by DFT calculations. We also thank Prof. K. J. Hüttinger (University of Karlsruhe) for many fruitful discussions and

Dr. H. H. Carstensen (Colorado School of Mines) for his useful comments on the reaction mechanism.

## BIBLIOGRAPHY

1. Benzinger, W.; Becker, A.; Hüttinger, K. J. *Carbon* 1996, 34, 957.
2. Guisnet, M.; Magnoux, P. *Appl Catal* 1989, 54, 1.
3. Guisnet, M.; Magnoux, P. *Stud Surf Sci Catal* 1994, 88, 53.
4. Guisnet, M.; Magnoux, P. *Catal Today* 1997, 36, 477.
5. Savage, G. *Carbon-Carbon Composite*; Chapman & Hall: London, 1993.
6. Hüttinger, K. J. *Chem Vapor Deposition* 1998, 4, 151.
7. Norinaga, K.; Deutschmann, O.; Hüttinger, K. J. *Carbon* 2006, 44, 1790.
8. Norinaga, K.; Deutschmann, O. *Ind Eng Chem Res* 2007, 46, 3547.
9. Norinaga, K.; Hüttinger, K. J. *Carbon* 2003, 41, 1509.
10. Troe, J. *J Chem Phys* 1977, 66, 4745.
11. Troe, J. *J Chem Phys* 1977, 66, 4758.
12. Troe, J. *J Phys Chem* 1979, 83, 114.
13. Troe, J. *Ber Bunsen-ges Phys Chem* 1983, 87, 161.
14. Becker, A.; Hüttinger, K. J. *Carbon* 1998, 36, 177.
15. Deutschmann, O.; Tischer, S.; Kleditzsch, S.; Janardhanan, V. M.; Correa, C.; Chatterjee, D.; Mladenov, N.; Minh, H. D. *DETCHEM Software package*, 2.1 ed., Karlsruhe 2007, www.detchem.com, accessed December 1, 2007.
16. Warnatz, J.; Maas, U.; Dibble, R. W. *Combustion*, 3rd ed.; Springer-Verlag: Heidelberg, 2000.
17. Richter, H.; Howard, J. B. *Phys Chem Chem Phys* 2002, 4, 2038.
18. Andra, H.; Langhoff, T. A.; Schnack, E.; Hüttinger, K. J. *Fuel* 2001, 80, 1273.
19. Frenklach, M.; Wang, H. *Proc Combust Inst* 1991, 23, 1559.
20. Wang, H.; Frenklach, M. *Combust Flame* 1997, 110, 173.
21. Frenklach, M. *Phys Chem Chem Phys* 2002, 4, 2028.
22. Dagaut, P.; Boettner, J. C.; Cathonnet, M. *Int J Chem Kinet* 1990, 22, 641.
23. Dean, A. M. *J Phys Chem* 1990, 94, 1432.
24. Dagaut, P.; Cathonnet, M.; Boettner, J. C. *Int J Chem Kinet* 1992, 24, 813.
25. Davis, S. G.; Law, C. K.; Wang, H. *Combust Flame* 1999, 119, 375.
26. Descamps, C.; Vignoles, G. L.; Feron, O.; Langlais, F.; Lavenac, J. *J Electrochem Soc* 2001, 148, 695.
27. Matheu, D. M.; Dean, A. M.; Grenda, J. M.; Green, W. H. *J Phys Chem A* 2003, 107, 8552.
28. Ziegler, I.; Fournet, R.; Marquaire, P. M. *J Anal Appl Pyro* 2005, 73, 212.
29. Ziegler, I.; Fournet, R.; Marquaire, P. M. *J Anal Appl Pyro* 2005, 73, 231.
30. Matheu, D. M.; Grenda, J. M. *J Phys Chem A* 2005, 109, 5332.
31. Matheu, D. M.; Grenda, J. M. *J Phys Chem A* 2005, 109, 5343.